Degree of Initial Hole Localization/Delocalization in Ionized Water Clusters[†]

Piotr A. Pieniazek, Eric J. Sundstrom,[‡] Stephen E. Bradforth, and Anna I. Krylov*

Department of Chemistry, University of Southern California, Los Angeles, California 90089-0482

Received: December 15, 2008; Revised Manuscript Received: February 2, 2009

The electronic structure of ionized bulk liquid water presents a number of theoretical challenges. Not the least of these is the realization that the detailed geometry of the hydrogen bonding network is expected to have a strong effect on the electronic couplings between water molecules and thus the degree of delocalization of the initially ionized system. This problem is approached from a cluster perspective where a high-level coupled cluster description of the electronic structure is still possible. Building on the work and methodology developed for the water dimer cation [*J. Phys. Chem. A* **2008**, *112,* 6159], the character and spectrum of electronic states of the water hole and their evolution from the dimer into higher clusters is presented. As the time evolution of the initially formed hole can in principle be followed by the system's transient absorption spectrum, the state spacings and transition strengths are computed. An analysis involving Dyson orbitals is applied and shows a partially delocalized nature of states. The issue of conformation disorder in the hydrogen bonding geometry is addressed for the water dimer cation.

1. Introduction

The properties of liquid water are known throughout a wide range of thermodynamic conditions, and many of these properties can be individually reproduced by using theoretical models, although a unified model is still elusive.[1] One such property of water, the electronic structure of the bulk liquid, particularly as it relates to the excited and ionized states, is still highly controversial and theoretical models that reproduce key experimental observables are not available.[2]

The structure of the valence band is of direct relevance in its ionization chemistry.[2] Although the ionization process has been investigated extensively since the 1960s, the initial stages are still not clearly understood. What is known is that within 1 ps, a thermalized electron, hydroxyl radical, and hydronium ion are formed within a few nanometer radius sphere; however, their yields and spatial distributions are strongly dependent on the initial energy deposited.[2,3] It is believed that water once stripped of an electron achieves final localization of the hole by downhill proton transfer to yield a H_3O^+, OH pair. The proton transfer is believed to be complete within 100 fs and can be followed by transient electronic spectroscopy,[4] although clear-cut evidence for this transformation has been hard to establish. This study aims to address the nature of the initially formed hole, $H_2O^+_{(aq)}$, formed on vertical ionization of bulk water at equilibrium. Depending on the nature of this initial state in the bulk, the subsequent proton transfer reaction may be characterized by different time scales and qualitatively different spatial distributions of the three resulting particles, the hydronium ion, OH radical, and solvated electron.[3] In turn, this will give different yields of radicals escaping geminate recombination, which lead to chemical damage.

In the condensed phase, water can be described as a rapidly fluctuating and partially disordered lattice of coupled chromophores, defined as individual water molecules, whose electronic states in turn correspond to the states of the gas phase

molecule. In such a system, two ionization scenarios can be imagined.[5–11] The first corresponds to the case when the electronic coupling between the water molecules is larger than the energy spread between them induced by different local environments. In this case the positive charge will be delocalized over many water molecules in the hydrogen bonded network, and the subsequent nuclear dynamics would lead first to the localization of the positive charge at a single site and then the proton transfer reaction. Alternatively, one can imagine that the energy spread between the different sites (diagonal disorder) exceeds the coupling. In such a case, the eigenstates will predominantly have a local character, and the proton transfer chemistry will ensue in a single step at the localized ionization site. Additionally, the degree of state localization will vary from state to state, giving rise to energy dependence of ionization characteristics.[12] Many of these issues can in principle be addressed by considering small water clusters with different hydrogen bonding geometries.

Earlier work on water cluster cations rarely addressed the nature of the vertically formed hole, beyond the early dimer controversy.[13–22] A notable exception is the study of Müller,[23] who investigated delocalization in small cyclic structures. Our previous work[24] on water dimer cation suggested strong couplings between the states of the H-bond donor and acceptor. The H-bond donor/acceptor moieties are defined as proton donor/acceptor. Two coupling pathways, both involving the a_1 orbital, have been observed. The a_1 orbital is capable of coupling with the b_1 orbital of the H-bond acceptor, as well as the b_2 orbital of the donor; although the extent of the interaction depends on the orientation of the two molecules, the previous study was restricted to the C_s symmetry structure. However, in the condensed phase a wide range of dimer geometries is sampled. Similar effects of the bulk on the electronic spectrum of water and the radiolysis products have also been theoretically investigated in cluster studies.[25–27]

Moreover, it is important to note that in the context of liquid water, the water dimer represents an extremely asymmetric arrangement of water molecules. In the bulk, a single water molecule is likely to serve both as an H-bond donor and

---

* Address correspondence to this author.
[‡] Current address: Department of Chemistry, UC Berkeley.

acceptor. The present study addresses both issues by considering other dimer configurations and larger clusters. The degree of charge delocalization in each case is quantified by using the Natural Bond Orbital (NBO) analysis.[28] We also address the reliability of the Koopmans ionization picture[29] by using the correlated Dyson orbitals.[30,31] In a system with many degenerate states correlation may play an important role in determining the electron distribution causing the breakdown of the Hartree−Fock molecular orbitals (MOs) based picture of ionization.

Computational studies of water ionization are complicated by the fact that the ionization of small water clusters typically occurs from the surface water molecules that are not H-bond acceptors, as dictated by electrostatic considerations, i.e., ionization from an H-bond acceptor places a positive charge near the proton of the H-bond donor. On the other hand, the positive charge is stabilized by the negatively charged oxygen of the other water molecule acting as a proton acceptor. In a dimer, the IE of the H-bond donor is lowered by 0.9 eV, while the IE of the H-bond acceptor increases by 0.6 eV.

Also, the nature of the cluster orbitals is difficult to assign, as they are mixtures of monomer orbitals of different symmetry. Moreover, the extent of mixing of different chromophore states is a function not only of the coupling element, but also of the diabatic separation. In an approximately tetrahedral network of water/ice all chromophores are nearly equivalent, and differences between them are likely to be induced by thermal fluctuations. In a cluster, water molecules are in different surroundings, regardless of the cluster size. This kind of diabatic separation is not present in the condensed phase.

Despite the inherent problems, cluster species are amenable to a detailed analysis and high-level ab initio calculations. The basic coupling pathways observed and quantified in the cluster will most likely still be present in the condensed phase. However, the cluster calculations account only approximately for the diagonal disorder. With these caveats in mind, we have conducted a series of studies designed to get us closer to issues in the bulk, while maintaining a high quality description of the electronic structure. We have explored the angular dependence of the electronic states of the water dimer cation at the vertical neutral geometry. We also studied the electronic states in three trimer geometries corresponding to three different H-bonding situations, as well as the electronic states of a tetrahedral water pentamer. Our emphasis has been on the degree of delocalization in the various states as well as the sensitivity of the electronic absorption spectrum of the vertically formed hole to conformation and cluster size.

2. Computational Details

The geometry of the simple $(H_2O)_2$ was optimized with MP2/6-311++G**. For the remaining clusters we start with a 17-mer, the geometry of which is taken from ref 32. This is the smallest stable water cluster for which an interior water molecule is present. This 17-mer structure was reoptimized with MP2/6-311++G**. Subsequently an interior pentamer, shown in Figure 1, was carved out but not reoptimized. Additionally, three trimer structures, corresponding to three different bonding situations, were cut out of the pentamer. In DD (fragments 1, 2, 3) and AA (fragments 1, 4, 5) structures the central water molecule acts only as an H-bond donor and acceptor to two other moieties, respectively. In the AD geometry (fragments 1, 3, 4) the central water acts both as a donor and an acceptor of a H-bond.

The ionized states derived from the three highest water monomer orbitals were characterized for each cluster by using

Figure 1. MP2/6-311++G** optimized geometry of the water pentamer. DD (fragment 1, 2, 3), AA (fragments 1, 4, 5), and AD (fragments 1, 3, 4) trimers were carved out for detailed study.

equation-of-motion coupled-cluster for ionization potentials with single and double substitutions (EOM-IP-CCSD)[33−36] and a 6-311++G** basis set. All electrons were correlated. As shown in ref 24, increasing the basis set to aug-cc-pVTZ affects IEs of H_2O, OH^-, and H_3O^+ by up to 0.3 eV resulting in better agreement with the available experimental values. Similar basis set effects were observed in larger systems, e.g., ionized uracil and uracil dimers.[37] However, we found that the basis set has little effect on the character of the EOM-IP wave functions, which are dominated by Koopmans-like contributions, and, consequently, on the properties that depend on electron distribution. For example, oscillator strengths of the transitions between ionized states of uracil computed with 6-31(+)G* and cc-pVTZ are within 2% from each other.

The charge on individual fragments was calculated using NBO analysis with fully relaxed density matrices defined for correlated wave functions.[38,39] The character of MOs was assigned based on visual inspection.

To characterize the dependence of dimer states on the relative orientation of the fragments in the dimer an angular scan was performed. The H-bond donor molecule was rotated around the oxygen−oxygen axis from 0° to 180° in 10° increments. The Dyson orbital was computed for all the trimer and the pentamer geometries. The weight of a given MO in the Dyson orbital is given by:

$$c_p{}^2 = \langle \Psi^N | p^+ | \Psi^{N-1} \rangle^2 \qquad (1)$$

where p^+ creates an electron in orbital p, and Ψ^N and Ψ^{N-1} are the N and $N-1$ electron wave functions described by CCSD and EOM-IP-CCSD, respectively. Trimer Dyson orbitals were obtained with the 6-311++G** and aug-cc-pVTZ basis sets. The results were nearly identical, and thus only the former basis set was chosen for the pentamer calculations.

It should be noted that describing charge localization in open-shell systems is a nontrivial task, often complicated by artifactual symmetry breaking and spin-contamination. Moreover, a high density of electronic states poses additional challenges. EOM-IP-CCSD overcomes these difficulties by using a well-behaved closed-shell reference wave function and a linear parametrization of the excitation operator. It describes multiple interacting electronic states in a balanced fashion, and accurately reproduces charge localization patterns in different electronic states.[40,41]

All ab initio calculations were performed by using the Q-CHEM ab initio package.[42] The basis sets were obtained from the EMSL repository.[43] Geometries of the trimers and the pentamer are available as Supporting Information.

3. Results and Discussion

3.1. Dimer. Dimer and monomer states can be conveniently related by using an an appropriate MO nomenclature. Following our DMO-LCFMO (Dimer Molecular Orbital−Linear Combi-

Hole Localization/Delocalization in Water Clusters
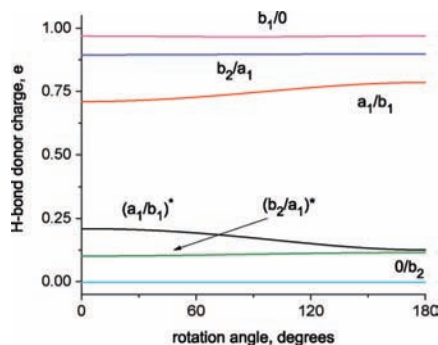
J. Phys. Chem. A, Vol. 113, No. 16, 2009 **4425**

Figure 2. Natural charge on the H-bond donor fragment in water dimer cation in the six lowest electronic states. Rotation is around the oxygen−oxygen axis, and angle 0° corresponds to the neutral dimer configuration. All calculations were done with EOM-IP-CCSD/6-311++G**.

nation of Fragment Molecular Orbitals) approach,[24,39,44] a composite notation of the form (H-bond donor MO)/(H-bond acceptor MO) is used to describe the dimer MOs. An asterisk signifies an antibonding character of the orbital with respect to the fragments. This notation directly gives the wave functions of the corresponding 1-electron system needed in understanding the spectroscopy. The relevant monomer orbitals in order of decreasing energy are b_1 (out-of-plane lone pair), a_1 (in-plane lone pair), and b_2 (σ_{OH}). They give rise to the 6 highest MOs of the dimer considered here (shown in Figure 3 from ref 24).

Molecules in the condensed phase sample a wide range of configurations. Since orbital overlap is known to play an important role in determining the diabatic coupling, it can be expected to also affect the character of the dimer wave function. This will result in a change of charge distribution and spectroscopy. Figure 2 presents the natural charge on the H-bond donor fragment in the dimer cation as a function of the rotation around the oxygen−oxygen axis. The charge distribution in the dimer cation appears to be relatively insensitive to the structure of the system. Rotation around the oxygen−oxygen axis lowers the symmetry of the system from C_s to C_1. Under the latter symmetry mixing of all states and significant changes in their character relative to the neutral configuration are formally possible, but do not occur. The lowest ionization is from the $b_1/0$ orbital and is constrained to the H-bond donor molecule. Largest changes in mixing with rotation are observed for the (a_1/b_1) and $(a_1/b_1)*$ pair of orbitals, but a visual MO inspection revealed only minor changes in the MO structure.

Figure 3 shows the excitation energy and transition dipole moment along the rotation angle for the five lowest electronic transitions. All these transitions are derived by exciting from a doubly occupied orbital to the $b_1/0$ SOMO (singly occupied molecular orbital). The effect on excitation energies is small, but pronounced changes in the intensity are observed. In particular, the $(b_1/0) \leftarrow (a_1/b_1)$ and $(b_1/0) \leftarrow (a_1/b_1)*$ transitions have much higher intensity at 90° than at 0°, as follows from the analysis of the natural charge of the ground and excited ion states. This is further supported by a visual inspection of MOs. This signifies an increase in the intermolecular contribution to the intensity. At the neutral configuration, the b_1 orbitals on the H-bond donor and acceptor fragments are perpendicular, and consequently the transition dipole moment is small. Rotation of the donor fragment by 90° makes the MOs parallel to each other, resulting in a large dipole moment coupling due to the close proximity of the orbitals. The intensities are nearly symmetric around 90°, implying that the direction of the hydrogen does not matter.
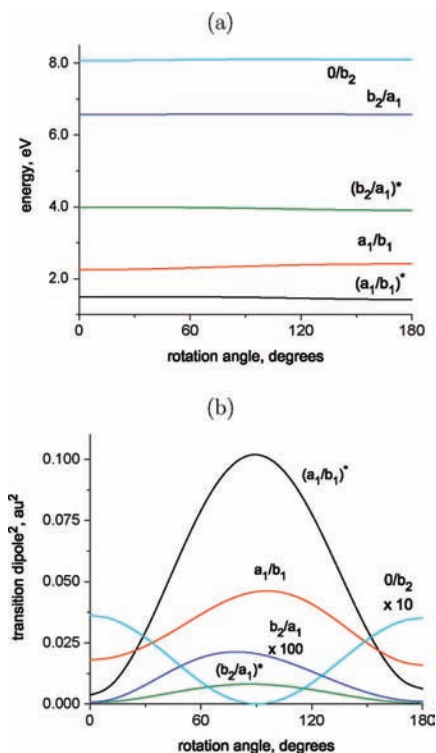

Figure 3. (a) Excitation energies and (b) transition dipole moments in water dimer cation. Rotation is around the oxygen−oxygen axis, and the angle 0° corresponds to the neutral dimer configuration. All calculations were done with EOM-IP-CCSD/6-311++G**.

Overall, we observe that the fragment composition of the states and excitation energies vary mildly with the rotation angle. This is in contrast to the transition properties, which in some cases change dramatically. The origin of this lies in the approximately spherically symmetric character of water MOs around the OH bond. Due to this shape, rotating around the oxygen−oxygen axis or changing the H-bond angles within a reasonable range only weakly affect the wave function in the interfragment region. It is the interactions in this region that determine the diabatic coupling. Intensity can stem from parts of the wave functions whose relative orientation changes significantly upon rotation, as illustrated in the previous paragraph.

3.2. Trimer. The IEs, fragment charges, and transition properties for the DD, AA, and AD trimers are given in Tables 1−3, respectively. The charge on the central molecule in the ionized states is shown in Figure 4. Before proceeding, we investigate the validity of the Koopmans picture. The ordering of the correlated states is the same as that of the MOs, and the square weights of the Hartree−Fock MO in the Dyson orbital are all close to 1. This means that the uncorrelated neutral orbital accurately describes the spatial extent of the hole. Increasing the basis set from 6-311++G** to aug-cc-pVTZ results in almost no change of the leading Dyson coefficient. Similar conclusions are drawn from the analysis of the R_1 amplitudes of the EOM-IP-CCSD wave functions: the smallest value of the leading amplitude corresponding to the Koopmans hole was 0.95. However, the differences between correlated and Koopmans IEs are significant (e.g., more than 1 eV).

In this analysis of state character we focus on the central water fragment and pay particular attention to whether the coupling pathways observed in the dimer are effective in explaining the observed state characteristics. When the central water molecule acts as a double donor (DD trimer), the ground state of the

TABLE 1: Leading Dyson MO Weights, Ionization Energies, Fragment Charges, Transition Dipoles, and Oscillator Strengths for the 9 Lowest States of the DD Water Trimer Cation[a]

	$c_p^{2\ b}$	c_p^2	IE	q_1	q_2	q_3	q_4	q_5	μ	f
1	0.999	0.998	10.375	0.885	0.057	0.058				
2	0.998	0.996	11.776	0.527	0.237	0.236			0.0187	6.42×10^{-4}
3	0.998	0.996	12.365	0.048	0.489	0.463			0.0182	8.88×10^{-4}
4	0.997	0.994	13.460	0.250	0.360	0.390			0.0179	1.35×10^{-3}
5	0.998	0.996	14.728	0.003	0.545	0.452			5.42×10^{-3}	5.78×10^{-4}
6	0.997	0.994	15.119	0.027	0.441	0.532			2.29×10^{-3}	2.66×10^{-4}
7	0.998	0.996	16.990	0.720	0.136	0.144			8.00×10^{-4}	1.30×10^{-4}
8	1.000	1.000	19.047	−0.044	0.998	0.046			5.22×10^{-3}	1.11×10^{-3}
9	1.000	0.999	19.096	−0.044	0.045	0.999			5.46×10^{-3}	1.17×10^{-3}

[a] The transition properties are relative to state number 1. q_1 is the charge on the central fragment. Results were obtained with EOM-IP-CCSD/6-311++G**. [b] Obtained with the aug-cc-pVTZ basis set.

TABLE 2: Leading Dyson MO Weights, Ionization Energies, Fragment Charges, Transition Dipoles, and Oscillator Strengths for the 9 Lowest States of the AA Water Trimer Cation[a]

	$c_p^{2\ b}$	c_p^2	IE	q_1	q_2	q_3	q_4	q_5	μ	f
1	0.998	0.995	11.451	0.065			0.335	0.600		
2	0.998	0.995	11.588	0.067			0.596	0.336		
3	0.990	0.977	13.157	0.482			0.256	0.262		
4	0.998	0.995	13.614	0.175			0.369	0.456	5.36	0.0601
5	0.987	0.970	14.239	0.541			0.278	0.181	2.59	0.0687
6	0.988	0.974	16.081	0.649			0.166	0.185	0.222	0.0159
7	0.996	0.991	17.911	0.138			0.429	0.433	0.295	0.0344
8	0.988	0.973	18.409	0.332			0.340	0.328	0.273	0.0351
9	1.000	0.999	19.988	1.016			−0.007	−0.009	2.93×10^{-3}	4.90×10^{-4}

[a] The transition properties are relative to state number 3. q_1 is the charge on the central fragment. Results were obtained with EOM-IP-CCSD/6-311++G**. [b] Obtained with the aug-cc-pVTZ basis set.

TABLE 3: Leading Dyson MO Weights, Ionization Energies, Fragment Charges, Transition Dipoles, and Oscillator Strengths for the 9 Lowest States of the AD Water Trimer Cation[b]

	$c_p^{2\ a}$	c_p^2	IE	q_1	q_2	q_3	q_4	q_5	μ	f
1	0.999	0.998	10.910	0.025		0.040	0.935			
2	0.993	0.985	11.939	0.812		0.063	0.126			
3	0.985	0.961	12.816	0.329		0.391	0.280		0.9932	0.0214
4	0.986	0.962	13.355	0.077		0.503	0.419		1.37	0.0475
5	0.993	0.985	14.613	0.534		0.318	0.148		0.0927	6.07×10^{-3}
6	0.996	0.991	15.682	0.129		0.860	0.012		0.0134	1.23×10^{-3}
7	0.993	0.985	17.346	0.138		0.045	0.817		0.484	0.0642
8	0.996	0.992	18.417	0.866		0.136	−0.002		3.56×10^{-3}	5.64×10^{-4}
9	0.999	0.999	19.708	0.007		1.013	−0.020		5.48×10^{-3}	1.04×10^{-3}

[a] The transition properties are relative to state number 2. q_1 is the charge on the central fragment. Results were obtained with EOM-IP-CCSD/6-311++G**. [b] Obtained with the aug-cc-pVTZ basis set.
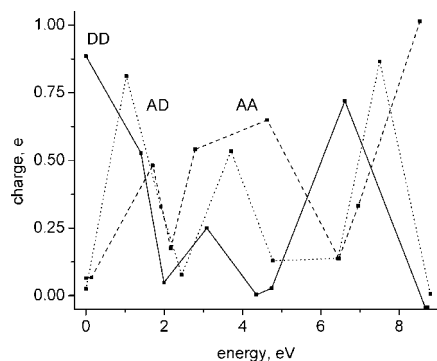

Figure 4. NBO charge on the central molecule in the three configurations of the water trimer. All calculations were done with EOM-IP-CCSD/6-311++G**.

cluster remains localized on the central fragment. Also in the dimer the H-bond orbital of the donor did not mix with acceptor orbitals. Excited states of this cluster are more delocalized than the ground state. No state can be assigned to ionization from the a_1 orbital, as it is dissolved in the b_1 ionizations of the

H-bond acceptors. The b_2 state remains rather localized. Finally, the highest two states are the ionizations from the b_2 MOs of the acceptors. As seen in the dimer, these states do not couple to the donor. Due to the approximate C_{2v} symmetry of the cluster all states, except acceptor b_2 states, are equally shared between the acceptor fragments.

In the AA isomer the central molecule acts only as an acceptor. The first two states correspond to ionization of the surface water molecules, following the electrostatic arguments from the Introduction. The b_1 and a_1 orbitals become dissolved and at most 50% of the electron density is located on the central fragment. Delocalization proceeds through the a_1 and b_2 of the donor. Similarly to the dimer, the b_2 remains fully localized. States involving ionization of peripheral fragments are mixtures of ionizations from the two monomers, as is the case in the DD trimer. The approximate C_{2v} cluster symmetry is also operational in this case. It is interesting to observe that the transitions in the AA trimer are typically larger than those in the two other cases. This is presumably caused by the delocalization, which gives rise to interfragment terms in the intensity expressions.

Hole Localization/Delocalization in Water Clusters

J. Phys. Chem. A, Vol. 113, No. 16, 2009 **4427**

TABLE 4: Leading Dyson MO Weights, Ionization Energies, Fragment Charges, Transition Dipoles, and Oscillator Strengths for the 15 Lowest States of the Water Pentamer Cation[a]

	c_p^2	IE	q_1	q_2	q_3	q_4	q_5	μ	f
1	0.992	11.031	0.007	0.041	0.042	0.108	0.803		
2	0.991	11.224	0.010	0.040	0.042	0.793	0.114		
3	0.987	11.823	0.747	0.064	0.061	0.061	0.066		
4	0.986	12.519	0.293	0.269	0.171	0.115	0.152	0.603	0.0103
5	0.995	12.964	0.048	0.507	0.473	−0.017	−0.011	0.107	3.00×10^{-3}
6	0.943	13.398	0.050	0.150	0.205	0.006	0.590	1.22	0.0470
7	0.946	13.557	0.071	0.134	0.196	0.607	−0.009	0.784	0.0333
8	0.979	14.735	0.286	0.265	0.230	0.109	0.110	0.0969	6.92×10^{-3}
9	0.995	15.231	0.019	0.593	0.424	−0.018	−0.018	5.43×10^{-3}	4.53×10^{-4}
10	0.975	15.746	0.150	0.279	0.504	0.029	0.037	1.06×10^{-3}	1.02×10^{-4}
11	0.990	17.390	0.058	0.043	0.047	0.304	0.547	0.410	0.0560
12	0.966	17.732	0.139	0.057	0.051	0.493	0.260	0.220	0.0319
13	0.995	18.358	0.769	0.116	0.127	0.002	−0.014	7.97×10^{-3}	1.28×10^{-3}
14	0.998	19.423	−0.011	1.011	0.042	−0.023	−0.019	4.79×10^{-3}	8.91×10^{-4}
15	0.998	19.595	−0.011	0.041	1.012	−0.022	−0.020	6.01×10^{-3}	1.14×10^{-3}

[a] The transition properties are relative to state number 3. q_1 is the charge on the central fragment. Results were obtained with EOM-IP-CCSD/6-311++G**.

The AD isomer is the case when the central molecule acts both as an acceptor and a donor. This is a very interesting case, as formally all the orbitals have favorable interaction partners and can delocalize. Despite this, there is still a fair amount of localization in some states. The charge on the central molecule for the peak corresponding to b_1 ionization is 0.81, compared to 0.88 in the DD case. The b_2 charge is 0.87. The a_1 state, which has the possibility to couple both to donor and acceptor, has a 0.53 charge.

Overall, the coupling pathways observed in the dimer prove effective in rationalizing the trimer results. These are particularly efficient at dissolving states related to the a_1 monomer orbital. The trimer results also shed light on the lowering of water IE in the bulk. Condensed phase measurements by Winter and co-workers,[46] show that the IE decreases from 12.6 eV in the gas phase to 11.2 eV. The computed IE of an isolated water molecule is 12.3 eV. The geometry of the central molecule in the pentamer is distorted from its equilibrium C_{2v} configuration, changing the IE to 12.2 eV. Thus, the geometry distortion effect on IE is rather small. In DD mostly central first ionization is 10.4 eV. This is similar in magnitude to the effect observed in the bulk phase. In the AA isomer it is pushed up to 13.2 eV, although it is a stretch to assign it to the central moiety. Both effects coexist in the AD isomer, where the central IE is 11.9 eV. While still lower than the monomer value, the effect is not nearly as dramatic as that in the dimer or the other two trimers, where only stabilizing or destabilizing effect is present but not both. The large lowering of IE in bulk water is thus not a simple result of nearest-neighbor interactions, but occurs due to the extended dielectric response of the bulk phase.

3.3. Pentamer. Water pentamer results are shown in Table 4 and the charge on the central fragment is plotted in Figure 5. The Koopmans ionization picture still holds for this system, as evidenced by the leading Dyson MO coefficients. Natural charges reveal that significant delocalization occurs in all states and the ionization process involves removal of an electron from several molecules. The two lowest electronic states of the pentamer cation correspond to ionization of the surface molecules. Not a single state can be completely assigned to the central fragment; however, crude correlations can be established. States corresponding to the ionization from b_1 and b_2 orbitals localized on the central water can be discerned (states 3 and 13, respectively), but not from a_1. This is in agreement with the photoelectron and X-ray emission spectra of the liquid phase,
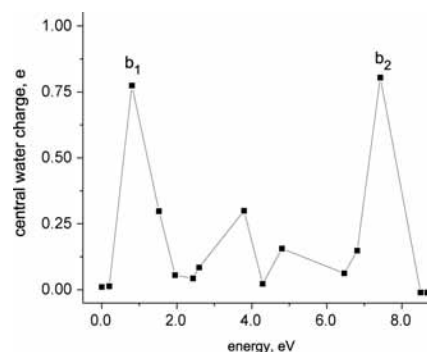

Figure 5. NBO charge on the central fragment in a water pentamer cation as a function of the excitation energy. All calculations were done with EOM-IP-CCSD/6-311++G**.

where the ionization/emission from the a_1 orbital is broadened compared to that of other orbitals.[45,46] This effect is attributed to the strong participation in the hydrogen bonding and the concomitant delocalization of a_1.

The state that is most localized on the central fragment has an ionization energy of 11.8 eV, 0.4 eV lower than the isolated monomer. Thus, even in this case the bulk limit is not reached.

3.4. Spectroscopy. The condensed-phase spectroscopy for the vertically ionized state can be modeled by considering excitations from the lowest state localized on the central cluster fragments. In other words, this state is taken to mimic the liquid ground states. This procedure can be performed both for the AD trimer (state 2) and the pentamer (state 3). The spectra are shown in Figure 6. First, consider the fate of the valence H_2O^+ in the cluster. In the gas phase the excitation energies of H_2O^+ are 2.0 ($a_1 \rightarrow b_1$) and 6.0 ($b_2 \rightarrow b_1$) eV. In the AD trimer these energies are shifted to the blue, 2.7 and 6.5 eV. It is more difficult to assign these transitions in the pentamer. The higher energy transition is at 6.5 eV. The a_1 state cannot be assigned. Tentatively, the most localized state in the a_1 region is at 2.9 eV. Thus, both excitations appear to shift to the blue. This is in agreement with the experimental difference of tentative vertical IEs, 2.3 and 6.3 eV.[46] The wide deviation in the a_1 energy is due to the uncertainties in the assignment rather than the error in the calculation.

Analysis of the pentamer and trimer fragment charges and transition intensities in Tables 3 and 4 reveals that the most prominent features in the spectra are in fact charge transfer transitions. These involve transfer of an electron to the central
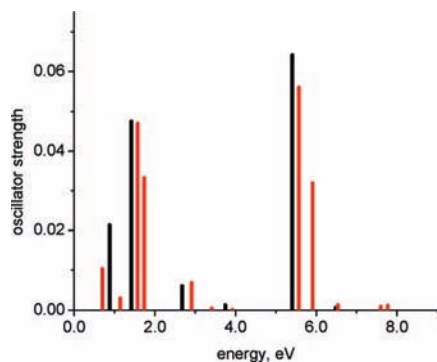
Figure 6. EOM-IP-CCSD/6-311++G** excitation energies and oscillator strengths for transitions from the state localized on the central moiety in the AD trimer (black) and the pentamer (red).

fragment and occur at lower excitation energies than the nearest localized transitions. Their intensity originates from two sources, the dipole moment coupling between the central fragment and the other moieties and the coupling between the electron density on the other moieties. The observed intensities are too large to be due to monomer intensity.

4. Conclusions

The present cluster study reveals that prior to nuclear relaxation, the hole produced by vertical ionization is partly delocalized, particularly when ionization involves removing an electron from an a_1-monomer-derived orbital. Typically, ionization of liquid water is pictured in terms of a creation of a b_1 hole to yield the ground electronic state of the cation. This is likely true for photoionization at most energies between 6 and 12 eV; however, it has recently been suggested that photoionization via excitation into the $\tilde{B}$ ($^1A_1$) state of liquid water, which promotes an a_1 electron, will lead initially to an a_1 hole.[12] The nearest neighbor couplings that give rise to this delocalization are already present in the dimer. The coupling not only causes delocalization, but also induces mixing of different cation states. Returning to the b_1 hole ground state of ionized water, the spectroscopic signature of the condensed phase appears very similar to that of the gas phase. Two broad bands appear at roughly similar positions. The biggest difference is in the acquired intensity, which comes mostly from the charge transfer component. The delocalized nature of the hole will also impact the dynamics of the ionization process. The delocalized hole is likely to persist until a fluctuation large enough to induce localization occurs and subsequently drives the proton transfer reaction to produce the OH radical. This final relaxation stage separates the spin and charge.

This study suggests that dimer and small cluster calculations may be useful in predicting the excitation energies of ionized bulk water. The calculated band positions are insensitive to the cluster size or the particular geometry. This is not true of the transition properties, which offer a probe of the structure and dynamics of the system. The main part of their intensity comes from the intermolecular character of the wave functions. Calculation of the associated intensities requires proper averaging over the thermally sampled configurations.

References and Notes

(1) Ball, P. *Science* **2008**, *452*, 291.
(2) Garrett, B. C.; Dixon, D. A.; Camaioni, D. M.; Chipman, D. M.; Johnson, M. A.; Jonah, C. D.; Kimmel, G. A.; Miller, J. H.; Rescigno, T. N.; Rossky, P. J.; Xantheas, S. S.; Colson, S. D.; Laufer, A. H.; Ray, D.; Barbara, P. F.; Bartels, D. M.; Becker, K. H.; Bowen, H.; Bradforth, S. E.; Carmichael, I.; Coe, J. V.; Corrales, L. R.; Cowin, J. P.; Dupuis, M.; Eisenthal, K. B.; Franz, J. A.; Gutowski, M. S.; Jordan, K. D.; Kay, B. D.; LaVerne, J. A.; Lymar, S. V.; Madey, T. E.; McCurdy, C. W.; Meisel, D.; Mukamel, S.; Nilsson, A. R.; Orlando, T. M.; Petrik, N. G.; Pimblott, S. M.; Rustad, J. R.; Schenter, G. K.; Singer, S. J.; Tokmakoff, A.; Wang, L. S.; Wittig, C.; Zwier, T. S. *Chem. Rev.* **2005**, *105*, 355.
(3) Elles, C. G.; Jailaubekov, A. E.; Crowell, R. A.; Bradforth, S. E. *J. Chem. Phys.* **2006**, *125*, 44515.
(4) Gauduel, Y.; Pommeret, S.; Migus, A.; Antonetti, A. *Chem. Phys.* **1990**, *149*, 1.
(5) Skinner, J. L. *J. Phys. Chem.* **1994**, *98*, 2503.
(6) Garcia, M. E.; Pastor, G. M.; Bennemann, K. H. *Phys. Rev. B* **1993**, *48*, 8388.
(7) Kurnikov, I. V.; Tong, G. S. M.; Madrid, M.; Beratan, D. N. *J. Phys. Chem. B* **2002**, *106*, 7.
(8) Shkrob, I. A.; Sauer, M. C., Jr.; Jonah, C. D.; Takahashi, K. *J. Phys. Chem. A* **2002**, *106*, 11855.
(9) Shkrob, I. A. *J. Phys. Chem. A* **2002**, *106*, 11871.
(10) Voityuk, A. A. *J. Chem. Phys.* **2005**, *122*, 204904.
(11) Santoro, F.; Barone, V.; Improta, R. *Proc. Natl. Acad. Sci.* **2007**, *104*, 9931.
(12) Elles, C. G.; Rivera, C. A.; Zhang, Y.; Pieniazek, P. A.; Bradforth, S. E. *J. Chem. Phys.* **2008**. In press.
(13) Moncrieff, D.; Hillier, I. H.; Saunders, V. R. *Chem. Phys. Lett.* **1982**, *89*, 447.
(14) Sato, K.; Tomoda, S.; Kimura, K. *Chem. Phys. Lett.* **1983**, *95*, 579.
(15) Curtiss, L. A. *Chem. Phys. Lett.* **1983**, *96*, 442.
(16) Tomoda, S.; Kimura, K. *Chem. Phys.* **1983**, *82*, 215.
(17) Curtiss, L. A. *Chem. Phys. Lett.* **1984**, *112*, 409.
(18) Gill, P. M. W.; Radom, L. *J. Am. Chem. Soc.* **1988**, *110*, 4931.
(19) Sodupe, M.; Oliva, A.; Bertran, J. *J. Am. Chem. Soc.* **1994**, *116*, 8249.
(20) Tachikawa, H. *J. Phys. Chem. A* **2004**, *108*, 7853.
(21) Tachikawa, H. *J. Phys. Chem. A* **2002**, *106*, 6915.
(22) Furuhama, A.; Dupuis, M.; Hirao, K. *J. Chem. Phys.* **2006**, *124*, 164310.
(23) Müller, I. B.; Cederbaum, L. S. *J. Chem. Phys.* **2006**, *125*, 204305.
(24) Pieniazek, P. A.; VandeVondele, J.; Jungwirth, P.; Krylov, A. I.; Bradforth, S. E. *J. Phys. Chem. A* **2008**, *112*, 6159.
(25) Chipman, D. M. *J. Chem. Phys.* **2006**, *124*, 044305.
(26) Chipman, D. M. *J. Chem. Phys.* **2005**, *122*, 044111.
(27) Chipman, D. M. *J. Phys. Chem. A* **2008**. In press.
(28) Weinhold, F.; Landis, C. R. *Chem. Educ.: Res. Pract. Eur.* **2001**, *2*, 91.
(29) Koopmans, T. *Physica* **1933**, *1*, 104.
(30) Cederbaum, L. S.; Zobeley, J. *Chem. Phys. Lett.* **1999**, *307*, 205.
(31) Oana, M.; Krylov, A. I. *J. Chem. Phys.* **2007**, *127*, 234106.
(32) Hartke, B. *Phys. Chem. Chem. Phys.* **2003**, *5*, 275.
(33) Sinha, D.; Mukhopadhyay, D.; Mukherjee, D. *Chem. Phys. Lett.* **1986**, *129*, 369.
(34) Sinha, D.; Mukhopadhya, D.; Chaudhuri, R.; Mukherjee, D. *Chem. Phys. Lett.* **1989**, *154*, 544.
(35) Chaudhuri, R.; Mukhopadhyay, D.; Mukherjee, D. *Chem. Phys. Lett.* **1989**, *162*, 393.
(36) Stanton, J. F.; Gauss, J. *J. Chem. Phys.* **1999**, *111*, 8785.
(37) Golubeva, A. A.; Krylov, A. I. *Phys. Chem. Chem. Phys.* **2009**, *11*, 1303.
(38) Stanton, J. F.; Gauss, J. *J. Chem. Phys.* **1994**, *101*, 8938.
(39) Pieniazek, P. A.; Bradforth, S. E.; Krylov, A. I. *J. Chem. Phys.* **2008**, *129*, 074104.
(40) Pieniazek, P. A.; Arnstein, S. A.; Bradforth, S. E.; Krylov, A. I.; Sherrill, C. D. *J. Chem. Phys.* **2007**, *127*, 164110.
(41) Krylov, A. I. *Annu. Rev. Phys. Chem.* **2008**, *59*, 433.

Hole Localization/Delocalization in Water Clusters

J. Phys. Chem. A, Vol. 113, No. 16, 2009 **4429**

(42) Shao, Y.; Molnar, L. F.; Jung, Y.; Kussmann, J.; Ochsenfeld, C.; Brown, S.; Gilbert, A. T. B.; Slipchenko, L. V.; Levchenko, S. V.; O'Neil, D. P.; Distasio, R. A., Jr.; Lochan, R. C.; Wang, T.; Beran, G. J. O.; Besley, N. A.; Herbert, J. M.; Lin, C. Y.; Van Voorhis, T.; Chien, S. H.; Sodt, A.; Steele, R. P.; Rassolov, V. A.; Maslen, P.; Korambath, P. P.; Adamson, R. D.; Austin, B.; Baker, J.; Bird, E. F. C.; Daschel, H.; Doerksen, R. J.; Drew, A.; Dunietz, B. D.; Dutoi, A. D.; Furlani, T. R.; Gwaltney, S. R.; Heyden, A.; Hirata, S.; Hsu, C.-P.; Kedziora, G. S.; Khalliulin, R. Z.; Klunziger, P.; Lee, A. M.; Liang, W. Z.; Lotan, I.; Nair, N.; Peters, B.; Proynov, E. I.; Pieniazek, P. A.; Rhee, Y. M.; Ritchie, J.; Rosta, E.; Sherrill, C. D.; Simmonett, A. C.; Subotnik, J. E.; Woodcock, H. L., III; Zhang, W.; Bell, A. T.; Chakraborty, A. K.; Chipman, D. M.; Keil, F. J.; Warshel, A.; Herhe, W. J.; Schaefer, H. F., III; Kong, J.; Krylov, A. I.; Gill, P. M. W.; Head-Gordon, M. *Phys. Chem. Chem. Phys.* **2006**, *8*, 3172.

(43) Basis sets were obtained from the Extensible Computational Chemistry Environment Basis Set Database, Version 1.2.2, as developed and distributed by the Molecular Science Computing Facility, Environmental and Molecular Sciences Laboratory, which is part of the Pacific Northwest Laboratory, P.O. Box 999, Richland, Washington 99352, and funded by the U.S. Department of Energy. The Pacific Northwest Laboratory is a multiprogram laboratory operated by Battelle Memorial Institute for the U.S. Department of Energy under contract DE-AC06-76RLO 1830. Contact David Feller or Karen Schuchardt for further information.

(44) Pieniazek, P. A.; Krylov, A. I.; Bradforth, S. E. *J. Chem. Phys.* **2007**, *127*, 044317.

(45) Guo, Y.; Luo, J.-H.; Augustsson, A.; Rubensson, J.-E.; Såthe, C.; Ågren, H.; Siegbahn, H.; Nordgren, J. *Phys. Rev. Lett.* **2002**, *89*, 137402.

(46) Winter, B.; Weber, R.; Widdra, W.; Dittmar, M.; Faubel, M.; Hertel, I. V. *J. Phys. Chem. A* **2004**, *108*, 2625.

JP811059Z